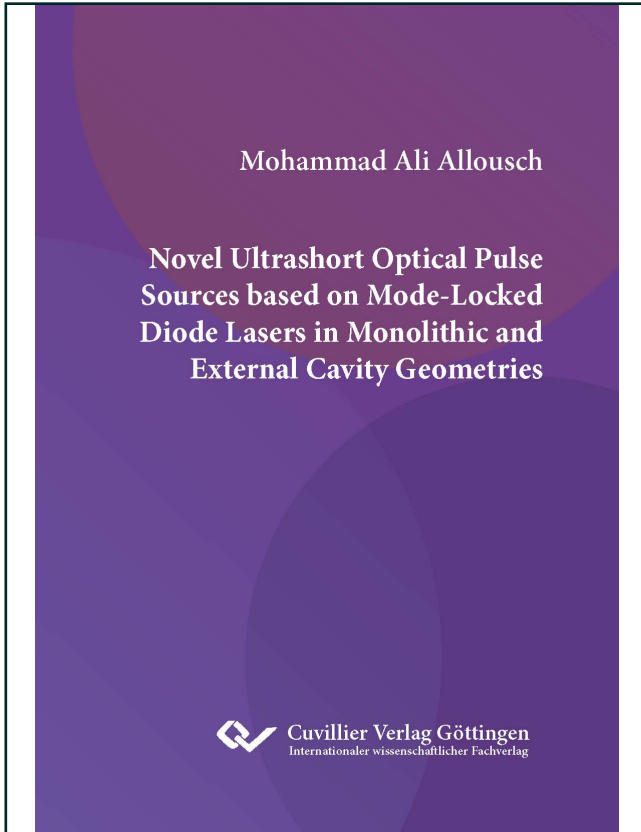




Mohammad Ali Allousch (Autor)

**NOVEL ULTRASHORT OPTICAL PULSE SOURCES BASED  
ON MODE-LOCKED DIODE LASERS IN MONOLITHIC  
AND EXTERNAL CAVITY GEOMETRIES**



<https://cuvillier.de/de/shop/publications/8961>

Copyright:

Cuvillier Verlag, Inhaberin Annette Jentzsch-Cuvillier, Nonnenstieg 8, 37075 Göttingen,  
Germany

Telefon: +49 (0)551 54724-0, E-Mail: [info@cuvillier.de](mailto:info@cuvillier.de), Website: <https://cuvillier.de>

# Chapter 1

## Introduction

By observing the development of high-technologies, it can be clearly revealed that manufacturing technologies tends towards compactness and cost-efficiency. Like any other technological field, laser industry has been massively developed over the past 30 years. This can be attributed to employing semiconductor lasers as prime candidates in several research and industrial domains. These domains involve for instance, ultrashort optical pulse generation and amplification, laser spectroscopy, and frequency comb generation. In the ultrashort pulse generation field, mode-locked diode lasers have demonstrated robustness, stability, and high-efficiency. They show cost-competitiveness and compact design which enable large volume production. Furthermore, their wavelength can be simply tailored during manufacturing by manipulating their gain materials, which in turn allows a broad wavelength range of the emitted light. In addition to mode-locked diode lasers, semiconductor optical gain materials are exploited in light amplification purposes, through the manufacturing of SOAs. Such amplifiers allow increasing the optical pulse-energy, towards compact, portable, and high-power laser accomplishment.

In this doctoral thesis, novel ultrashort optical pulse sources are presented based on mode-locked diode lasers, in both monolithic and external cavity configurations. These sources can be employed in various applications, such as THz TDS, clock sources in frequency synthesizers, two-photon microscopy, optical sampling, and comb generation for high-rate data transmission. The first work involves femtosecond pulse generation from external cavity diode laser based on self-mode-locking regime at wavelength range of 1550 nm. Due to the absence of non-linear saturable absorber element in self-mode-locked lasers, this laser hence allows exploiting the full gain of the semiconductor materials. Thus, optical pulses with pulse-width in femtosecond range are realized by propagating the pulses in a sufficient length of standard SMF-28. This work is extended by varying the external cavity length to correspond to multiple integer length of the employed gain chip. A novel observation is explored which reveals the suppression of all external cavity harmonics operation except the high harmonic which approximately corresponds to monolithic chip length. The laser can be consequently operated at adjustable high repetition-rate by fine tuning the length of the external cavity. The observed adjustable range corresponds to  $\pm 300$  MHz of the central repetition-rate. Femtosecond optical pulses are obtained with record pulse-to-pulse RMS timing jitter

of 2.4 fs. Secondly, a novelty systematic comparison between self-mode-locking and passive mode-locking operation of a monolithic quantum-dot laser chip at 1550 nm wavelength range is investigated. In both regimes, femtosecond optical pulses are obtained by employing a sufficient SMF-28 fiber length behind the laser chip. While self-mode-locking exhibits high pulse quality and broad optical frequency combs, passive mode-locking shows a limited gain bandwidth due to the employment of saturable absorber. Thirdly, optical frequency comb generation from self-mode-locked diode laser by the influence of external optical feedback, is investigated. Despite anti-reflection coated facet, the chip operates monolithic due to the absence of a suppression mechanism such as an enhanced waveguide geometry. Thus, a comparison based on the obtained frequency comb is conducted between monolithic and external cavity operation. The external optical feedback enables a frequency comb enhancements. Fourthly, noise, RF, and optical pulse analysis of a sub-GHz InP-based 1550 nm monolithic passively and hybrid mode-locked laser chip, are explored. This work represents the approaches which can be performed to explore timing jitter in laser chips while operating in passive and hybrid mode-locking regimes. It also shows the advantage of RF analysis of the laser chip and its mounting PCB, as a key for impedance matching circuit-design which is significant to maintain a high efficiency operation. Fifthly, resonant pulse amplification based on mode-locked diode laser at 850 nm wavelength range is investigated. Two laser cavities are built, one for optical pulse generation based on external cavity diode laser, and the other as a ring cavity which employs a tapered semiconductor amplifier as a gain element. By seeding the ring cavity with generated pulses and matching the length of both cavities, resonant pulses amplification is realized. Finally, a proof-of-principle two-photon microscopy based on femtosecond laser pulses generated from edge-emitting mode-locked diode laser at 850 nm is demonstrated. Optical pulses are generated from external cavity based master oscillator, subsequently amplified utilizing a power amplifier, and compressed at the end while propagating through an optical compressor. The investigated samples are microspheres which feature absorption / excitation lines at roughly 428 nm / 467 nm, respectively.

This thesis is structured in the following chapters. A fundamentals of laser, mode-locking, and noise is presented in the beginning. Then, each conducted experiment is presented separately along with the obtained results, and this is covered in chapters 2 to 9. In the end, a summery and outlook are presented.

All experimental setups employed in this doctoral thesis were solely built by M. Ali Allousch. Except for the conducted analysis of the measurements in 7.4, which were carried out by Marcel van Delden, all measurements and analysis in this thesis were performed by M. Ali Allousch. The PCBs utilized in this work were designed by M. Ali Allousch, and manufactured at the Electrical Engineering faculty at RUB.

# Chapter 2

## Fundamentals

In this chapter, an overview of the theoretical background behind the achieved results is outlined. The laser basics which involve the principle of laser and laser dynamics will be discussed. Ultrashort optical pulse generation will be explained. Principle of mode-locking including passive-mode-locking and hybrid mode locking, suppression of multiple pulse formation and timing jitter will be briefly introduced. Self-mode-locking, quantum-dot, and quantum-dash semiconductor lasers are presented. Brief description of the optical compressor will be discussed. Ultrashort optical pulse amplification along with spectral broadening phenomena will be covered. Single-pass amplifiers will be presented.

### 2.1 Laser Basics

In this section, laser definition and the main three components of the laser will be discussed. The general schematic of bulk and semiconductor lasers will be outlined afterwards. The principle of gain and losses will be explained. The modes in the optical resonator will be presented as well.

#### 2.1.1 Laser Definition

Laser = Light Amplification by Stimulated Emission of Radiation [2]

Laser is a source that emits coherent, monochromatic radiation in the optical zone of the electromagnetic spectrum [3]. It can be represented by an electronic oscillator which is considered as a source of RF. Such an oscillator involves an amplifier (active medium) followed by a feedback circuit as depicted in Figure 2.1.

As this active medium is supplied with power, it produces an amplification. The feedback can be an inductor, capacitor, or RC circuit. Analogous to the electronic oscillator, the laser includes of three main components. The active medium which features gain when it is pumped, pumping source and an optical feedback unit (optical resonator / cavity). The resonator exhibits a certain loss associated with it. Once gain exceeds loss, a net amplification is achieved and the laser commences oscillating.

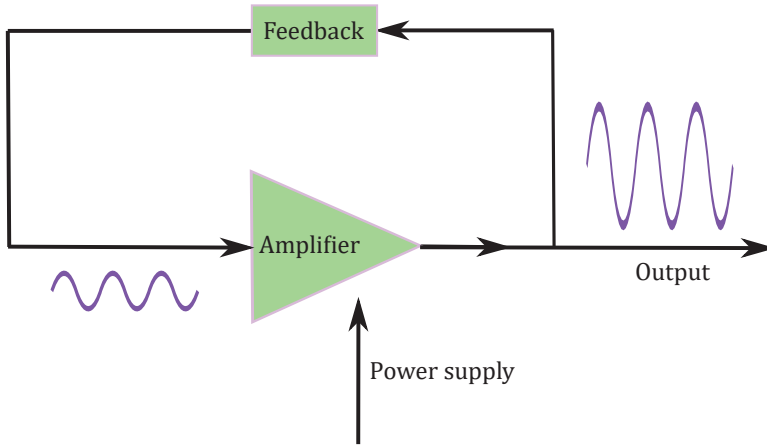


Figure 2.1: Electronic Oscillator = Amplifier + Feedback. The power supply represents the pumping source in the laser [1].

### 2.1.2 General Schematic of the Laser

Simple schematic of the bulk laser is illustrated in Figure 2.2. Nd:YAG laser as an example of the bulk laser is pumped externally by a diode laser or a flash lamp. The active medium is placed inside an optical cavity which is realized between two mirrors of reflectivity  $R_1$  and  $R_2$ .

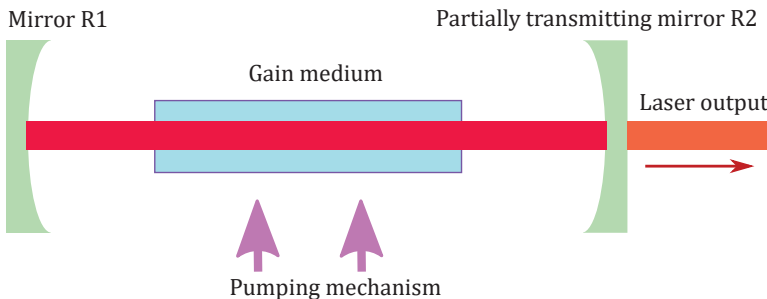


Figure 2.2: General schematic of bulk lasers. Laser components are: active medium, pumping source and optical cavity formed by  $R_1$  and  $R_2$  [1].

For semiconductor laser (SC), it has almost analogous structure. Figure 2.3 depicts a cross-section of the semiconductor laser [4]. It is pumped electrically with current streams in a forward biased p-n junction. Given a sufficiently massive injection current, the injected carrier concentration is hence large as can be concluded from the equation 2.1 [1]:

$$\Delta n = \frac{(i/e) \times \tau}{l \times w \times d} \quad (2.1)$$

where  $i$ : injection current,  $\tau$ : recombination time,  $w$  and  $d$ : width and height of the device and  $l$ : thickness of the active region. Consequently, the injected carrier concentration be considerable, the separation between Fermi-levels is then large enough to achieve a situation that  $E_{fc} - E_{fv} > E_g$ , where  $E_{fc}$  and  $E_{fv}$ : quasi-Fermi levels and  $E_g$ : bandgap energy. In this situation, a gain in the active medium can be obtained.

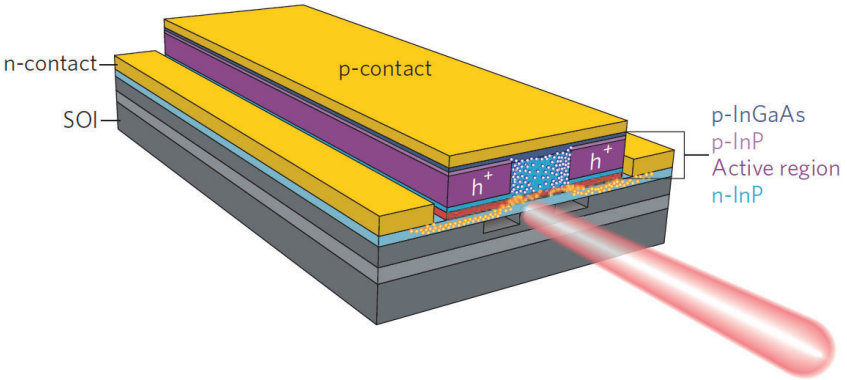


Figure 2.3: Cross section of the semiconductor laser. It is an example of an integrated laser on a Si-photonic platform. Laser components are: active medium of thickness  $l$ , electrical pumping and optical resonator formed by two cleaved facets [4].

To demonstrate the gain in simple terms, it will be outlined in the atomic system. Considering  $N_1$  and  $N_2$  as number of atoms per unit volume in the energy level  $E_1$  and  $E_2$ . Should the pumping be sufficiently hard, atoms will ascend from lower state to higher one. The gain is hence obtained, a situation of  $N_2 > N_1$  is accomplished and this process is called population inversion.

In bulk system, light is confined between two mirrors where it travels back and forth. These mirrors serve as an optical feedback since the same light is seeded into the active medium. In Figure 2.2, mirrors  $M_1$  and  $M_2$  feature a high reflectivity  $R_1 \approx 100\%$  and partially reflective  $R_2 \approx 95\%$ , respectively. Thus, part of the light emerges out of the cavity and constitutes the output light of the laser. It can be noticed that the mirrors are typically concave so that the beam waist is characterized by the mirror curvature radius as well as the length  $d$  between the mirrors (typically  $d$  is in the range of 10 cm for the Nd:YAG). In case a spherical mirrors resonator is realized, the modes of the resonator exhibit Hermite-Gaussian fields with the fundamental mode  $TEM_{00}$ . Hence, the field profile will have a Gaussian amplitude distribution [1].

Semiconductor (SC) laser reveals homogeneity to bulk lasers as the two ends of the SC chip are typically cleaved. In Figure 2.3, it is demonstrated that the SC medium features refractive indexes  $n_1$  and the other medium (air) introduces refractive index = 1. The emerged light reaches the cleaved end which exhibits a

reflectivity  $R$  described in equation 2.2. It is reflected afterwards to the other end and a feedback is subsequently formed. Considering  $n_1 = 3.6$ , 32% reflectivity is achieved, attributed the cleaved ends.

$$R = \left[ \frac{n_1 - 1}{n_1 + 1} \right]^2 \quad (2.2)$$

The mode in the SC laser is identified by the optical waveguide. The field in the active region exhibits a cosine distribution and outside (in the cladding) is exponentially decaying. The transverse modes in SC laser are characterized by the refractive indexes  $n_1$  and  $n_2$  as well as the thickness of the active region  $l$  [1].

### 2.1.3 Gain Coefficient in Semiconductor Lasers

To realize a gain from a SC, the gain coefficient  $\gamma_0$  must be greater than 0. To obtain that, the probability of emission  $f_e(\nu)$  must be greater than the probability of absorption  $f_a(\nu)$ . The gain coefficient is introduced by

$$\gamma_0(\nu) = \frac{\lambda^2}{8\pi\tau_r} \rho(\nu) f_g(\nu) \quad (2.3)$$

where  $\rho(\nu)$ : optical joint density of states,  $f_g(\nu)$ : Fermi inversion factor and  $\tau_r$ : effective spontaneous lifetime for stimulated emission. Given a positive  $f_g(\nu)$  ( $E_{fc} - E_{fv} > h\nu$ ), an amplification is consequently achieved.

Typical laser amplifiers are based on the quantum-well (QW) structure. Such a structure enables better confinement of the carriers in the active region due to the reduced thickness. An increase in the amplification gain and reduce in loss is thus achieved. Illustration of optical joint density of state in a QW structure can be seen in [1]. In comparison to bulk lasers where the density of state alters as the square root of energy, it remains constant from  $E_{g1}$  up to  $E_{g2}$  in QW structure. Once it reaches  $E_{g2}$  it features a hop and stays constant until  $E_{g3}$ . The amount of  $\rho(\nu)$  for the first constant line is  $\frac{2m_r}{\hbar l}$  and it will be doubled for the next constant line. The variation of  $\rho(\nu)$  is significant as the gain profile is defined by it. The  $f_g(\nu)$  depends on the quasi-Fermi levels and temperature, and it stays identical from QW and bulk lasers [1]. The plotted  $f_g(\nu)$  is for  $T > 0$  K. The  $\gamma_0(\nu)$  is outcome product of  $\rho(\nu)$  and  $f_g(\nu)$ . The gain coefficient of the QW laser features a narrower gain profile than the Bulk laser with a maximum gain  $\gamma_m = \frac{\lambda^2 m_r}{2\tau_r \hbar l}$ . By applying pumping to a certain level, almost a flat gain profile for a narrow amplification bandwidth will be obtained [1].

The gain profile of the single QW and bulk double-hetero-structure lasers as a function of the current density  $J$  is illustrated in [1]. It can be observed that the current density required to realize transparency  $J_T$  is smaller for the QW laser. Nevertheless, the gain in the single QW exhibits saturation at lower level. However, it boosts gradually in bulk laser case where it saturates at higher level [1].

### 2.1.4 Laser Dynamics: Gain and Losses

The basic laser theory at steady-state is to realize the gain in the active medium equal to the loss in the resonator. It can be observed that if the laser is pumped so that the condition  $E_{fc} - E_{fv} > E_g$  is maintained, the gain will exhibit the profiles represented in [5, 1]. Such profiles reflect the amounts of injected carrier concentration  $\Delta n$ . They determine the amplification bandwidth that corresponds to the frequency range at which the amplification is fulfilled. The amplification bandwidth broadens when the pumping is boosted. If the pump is not applied into the medium, an absorbing medium is thus realized and can be regarded as negative gain coefficient (serves as loss coefficient). Asymmetric gain curves are revealed in both QWs and bulk lasers [1].

The resonator loss originates from various sources, and can be characterized by the following: diffraction losses, scattering losses in the medium, and losses attributed to finite reflection of the mirrors [1].

$$\alpha_r = \alpha_s + \frac{1}{2d} \ln \left[ \frac{1}{R_1 R_2} \right] \quad (2.4)$$

where  $\alpha_s$ : diffraction and scattering losses; and it includes also re-absorption by non-inverted parts of the gain material,  $d$ : resonator length and  $R_1, R_2$ : mirrors reflectivity.

As mentioned above, gain should be equal to losses ( $\gamma = \alpha_r$ ) to realize an output light from the laser. The laser dynamics theory is presented as follow: once the oscillation commences, the gain coefficient should exceed the loss coefficient ( $\gamma > \alpha_r$ ). Consequently, all the frequencies within the bandwidth where the gain surpass the loss, will start oscillating. Given gain saturation demonstrated by [6], once gain exceeds losses; the gain curve will be dragged down by the system's dynamics. Hence, ( $\gamma = \alpha_r$ ) is achieved at the steady-state. This dynamics are called gain clamping [7], for which spectral hole-burning can be revealed [8] in the gain profile depending whether homogeneous or inhomogeneous broadening process occurs [1].

### 2.1.5 Modes in the Optical Resonator

Two types of modes are realized in optical resonators: longitudinal and transverse. While longitudinal modes identify the resonance frequencies, transverse modes identify to the field distribution. The round-trip phase shift is [1]:

$$k2d = q2\pi \quad (2.5)$$

where  $k$ : phase-shift coefficient,  $2d$ : round-trip distance (contains the refractive index of the medium) and  $q$ : integer number. It can be concluded from equation 2.5, that only these frequencies which fulfill a round-trip phase shift equal to integer multiple of  $2\pi$  will be maintained. These frequencies are called resonance frequencies and introduced in equation 2.6:

$$\nu_q = q\Delta f \quad (2.6)$$



where  $\Delta f = \frac{c}{2d}$ : resonance mode spacing.

Figure 2.4 illustrates the resonance frequencies in optical resonator. The gain

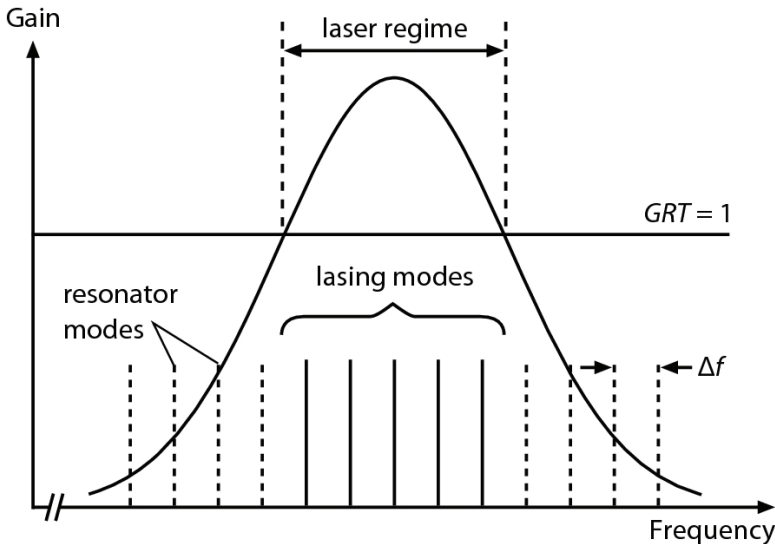


Figure 2.4: Illustration of the resonator modes. They are separated by the frequency  $\Delta f = \frac{c}{2d}$  [9].

bandwidth depicts all frequencies where the resonator exhibits net gain. However, only resonance frequencies that are located within the gain bandwidth and match the resonator round-trip phase condition, will build-up in the resonator. The rest of the resonance frequencies outside the gain bandwidth region will not grow as losses exceed gain in this region [1].

The field distribution profile along with the number of transverse mode in the SC laser are identified by the optical waveguide. The optical waveguide is characterized by the thickness  $d$  and the refractive indexes of active region and cladding. By choosing these parameters appropriately, a single transverse mode can be obtained. Based on the foregoing, single frequency laser is defined when a laser operates at a single longitudinal mode and single transverse mode [1].

## 2.2 External Cavity Diode Laser (ECDL)

Mode-locked diode laser based on monolithic chip geometry emits pulses with RR in the range of several gigahertz. The chip features two facets where their reflection is characterized depending on the application. To realize lower RRs at sub-gigahertz scheme, ECDL configuration is demanded. In the ECDL geometry, diode lasers are employed in extended cavity geometry by placing a mirror at a certain distance down-streaming of the diode laser. ECDL enables tuning RR

by altering the resonator length. The implemented laser chip features one anti-reflection (AR) coated facet. To realize the laser cavity, a lens is placed between the chip and the end mirror as illustrated in Figure 2.5. In mode-locked diode lasers, the chip exhibits a short section and a gain section. These sections allow realizing various mode-locking regimes depending on the applied parameters.

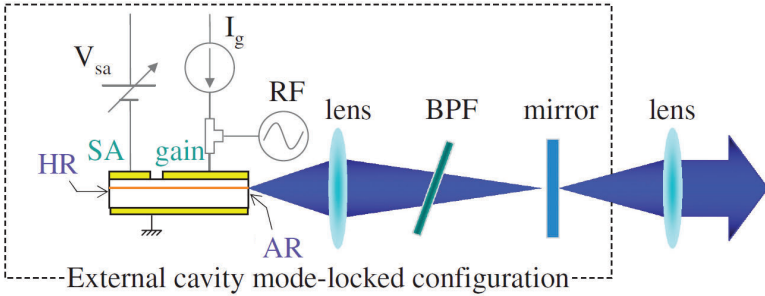


Figure 2.5: Illustration of an ECDL [10].

## 2.3 Ultrashort Optical Pulse Generation

Ultrashort pulses involve pulses with a pulse-width of a few tens of picosecond or mostly in the range of femtosecond. These pulses are typically obtained from mode-locked lasers. There are various ways to produce ultrashort pulses. Passive mode locking PML is one of these ways, which employs either saturable absorber inside the cavity [11, 12] or Kerr effect in the case of Ti:sapphire lasers [13]. In this section, the principle of mode locking will be outlined. Furthermore, PML, HML, and related phenomena such as multiple pulses formation and timing jitter will be presented. Moreover, self-mode-locking SML and quantum-dot semiconductor lasers will be briefly outlined.

### 2.3.1 Principle of Mode Locking

To generate ultrashort pulses, the energy in a laser resonator must be finite into a small spatial region. This demands realizing the optical power concentration into one solely fluctuation rather than being distributed among the whole set of fluctuations [14]. This is illustrated in Figure 2.4. The output is constituted by a sum of frequency components which correspond to the oscillating longitudinal modes. Thus, the electric field can be composed (without considering the spatial distribution) as

$$E(t) = \sum_m A_m \exp i[(v_0 + mv_F)t + \phi_m] \quad (2.7)$$

where  $A_m$  and  $\phi_m$  correspond to the amplitude and phase of the  $m$ th mode. Generally, the phases between the relative modes are randomly oscillating. When these

phases  $\phi_m$  are not forced to maintain a fixed relationship, the laser output will alter in time with random and systematic fluctuations. Hence, the average power will remain approximately equal to the simultaneous power [14, 15].

However, if the modes are forced to exhibit a fixed phase and amplitude relationship, for instance

$$\phi_m - \phi_{m-1} = \Delta\phi \quad (2.8)$$

the laser output will subsequently be a periodic function of time:

$$E(t) = A_0 \frac{\sin[(k+1)v_F t_1/2]}{\sin(v_F t_1/2)} \exp(iv_0 t) \quad (2.9)$$

where  $k$  is the number of locked modes,  $t_1 = t + \Delta\phi/v_F$ . Figure 2.6 illustrates the envelope of  $E^2(t)$  for specific number of  $k$ . The laser output is identified by a sequence of regularly spaced pulses. These pulses feature a width  $\Delta\tau$  approximately equal to  $1/\Delta\nu$  and the temporal periodicity of the pulses is identified as  $T = 2Ln/c$ . The number of locked modes,  $k$ , is characterized by the ratio of the pulse-width to the period. Depending on the envelope of the mode amplitudes, the pulse shape can be identified. This dynamic regime is called mode-locking. It can be realized in active, passive and hybrid techniques. Furthermore, it enables much shorter pulses to be generated compared to those revealed by gain switching or Q-switching [15, 14].

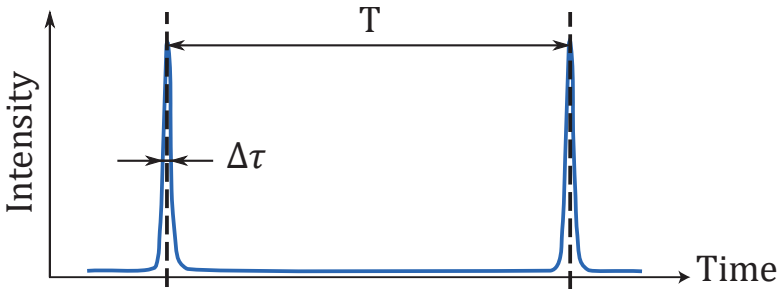


Figure 2.6: The envelope of  $E^2(t)$  for 7 locked modes is illustrated in this figure. Pulse-width is  $\Delta\tau$  and the pulses has a period  $T = 2Ln/c$  [16].

### 2.3.2 Passive and Hybrid Mode Locking

For realizing the laser oscillation from spontaneous fluctuations, the unsaturated gain has to exceed the unsaturated loss [15]. Implementing an appropriate nonlinear element that serves as saturable absorber into the laser resonator allows achieving passive mode locking [17]. Schematic setup of the passively mode-locked laser is illustrated in Figure 2.7.

The employed saturable absorber in SC lasers are slow type [19]. For achieving successful passive mode locking, considerable changes in both the gain and loss must be maintained while pulse propagation through the absorber. Furthermore,